Heliyon 10 (2024) e25520

Contents lists available at ScienceDirect

Heliyon

journal homepage: www.cell.com/heliyon

Research article

Biosynthesis of silver nanoparticles by banana pulp extract: Characterizations, antibacterial activity, and bioelectricity generation

Md Ohiduzzaman [a,b,**], M.N.I. Khan [c], K.A. Khan [a,d], Bithi Paul [e,*]

[a] Department of Physics, Jagannath University, Dhaka 1100, Bangladesh
[b] Department of Physics, Jashore University of Science and Technology, Jashore 7408, Bangladesh
[c] Materials Science Division, Atomic Energy Centre, Dhaka, Bangladesh
[d] Bangamata Sheikh Fojilatunnesa Mujib Science & Technology University, Jamalpur, Bangladesh
[e] Department of Physics, American International University-Bangladesh, Dhaka, Bangladesh

ARTICLE INFO

Keywords:
Biosynthesis
Pulp extract
Silver nanoparticles
Antibacterial activities
Bio-electrochemical cell

ABSTRACT

Here, green banana pulp extract (PE) has been used as a bio-reducing agent for the reduction of silver ions to silver nanoparticles (AgNPs). Bio-synthesized AgNPs were characterized by using UV, XRD, FEEM, TEM, and FTIR analysis. The face-centered cubic structures of AgNPs were formed with an average crystallite size of 31.26 nm and an average particle size of 42.97 nm. In this report, the electrical activities of green synthesized AgNPs have been evaluated along with the antibacterial activities. The antibacterial activities of AgNPs were evaluated against two pathogenic bacteria: *Escherichia coli* (gram-negative) *and Staphylococcus epidermidis* (gram-positive). AgNPs were added to the electrochemical cell and results demonstrated the improvement of power of the electrochemical cell. Green synthesized AgNPs showed excellent antibacterial activities against both gram-positive and negative bacteria and most importantly the NPs played an important role as an effective catalyst to enhance the electrical performance of bio-electrochemical cells. These significant findings may help in the advancement of nanotechnology in biomedical applications as well as in the creation of cheap and eco-friendly power generation devices.

1. Introduction

Nanotechnology focuses on creating and manipulating structures, devices, and systems at the nanoscale level, which ranges from 1 to 100 nm. The research on nanomaterials involves controlling the shape and size of materials to produce desired properties and functionalities [1–4]. Nano research is now being conducted in a wide range due to the developments of nanotechnology for multi-disciplinary applications [5,6]. Nanoparticles possess distinctive biological, optical, and electrical characteristics, making them useful in a wide range of applications. They are utilized in catalysis, drug delivery, biosensing, imaging, nanodevice manufacturing, and medicine due to these properties [7–10]. Researchers are very interested in noble metal nanoparticles among all nanomaterials because noble metals have various potential applications in the fields of physics, materials science, biology, chemistry, and medicine

* Corresponding author.
** Corresponding author. Department of Physics, Jagannath University, Dhaka 1100, Bangladesh.
E-mail addresses: ohid@just.edu.bd (M. Ohiduzzaman), chyabithi@gmail.com (B. Paul).

https://doi.org/10.1016/j.heliyon.2024.e25520
Received 30 November 2023; Received in revised form 24 January 2024; Accepted 29 January 2024
Available online 1 February 2024

[3,11,12]. Among all noble nanomaterials Ag nanoparticle is one of the most potential candidates due to its excellent electrical, optical, photocatalytic, antibacterial, and medicinal properties [12,13].

Nanoparticle synthesis follows key principles of green chemistry: opting for eco-friendly solvents, benign reducing agents, and non-toxic stabilizers [14]. Different physical and chemical methods have been used to synthesize the nanoparticles, but the toxicity of the chemicals used in the synthesis is a great concern in recent days [8,12]. Consequently, an eco-friendly bio-synthesis approach is now widely being used to fabricate nanoparticles where bio-reducing agents are used instead of chemical agents [15]. Several plant components, including extracts [16], fruit [17], bark [5,18], fruit peels [19], and roots [20] have been investigated thus far to produce silver, gold, platinum, and titanium nanoparticles in various sizes and shapes [5]. The secondary metabolites of plants such as flavonoids, and terpenoids play active roles as reducing, capping, and stabilizing agents during the reaction mechanism [7,21].

Recent years have seen a surge in green and microbial approaches—physical, chemical, biological, and enzymatic to discover bioactive nanoparticles [22,23]. Methods include using plant extracts, bacteria, fungi, algae, enzymes, and polymers [24,25]. Among these, mycogenic synthesis is well-documented. Plant extracts, acting as reducing and capping agents, are crucial in forming these green nanoparticles. Their metabolites play a vital role in characterizing and shaping these bioactive particles. The synthesis typically involves combining aqueous extract with a metal salt solution at room temperature, completing within short periods [25–27].

Silver nanoparticles are widely used across various industries like clothing, dentistry, photography, surgical devices, textiles, catalysis, optics, electronics, mirrors, prostheses, food production, cosmetics, agriculture, and more due to their versatile applications [28–30]. These nanoparticles, especially when synthesized through eco-friendly methods, exhibit diverse biological functions that make them valuable for treating diabetes, inflammation, cancer, infections, malaria, and as catalysts or sensors [25,31,32].

The escalating issue of antibiotic resistance has prompted researchers to seek affordable ways to create new antimicrobial agents [33]. Silver NPs combat microorganisms by damaging their negatively charged cell walls, disrupting membrane permeability, deactivating enzymes, and ultimately causing cell lysis and death [34]. The effectiveness of AgNPs relies on monovalent ionic silver (Ag^{+}), which penetrates microbial cells, inhibiting their growth by impeding respiratory enzymes and electron transport mechanisms [35,36]. Additionally, AgNPs influence cellular membrane permeability [37].

Hence, there's a growing emphasis on developing environmentally friendly, safe, and cost-effective biological approaches for producing nanoparticles (NPs) that pose no threat to life. Recent studies have highlighted the synthesis of AgNPs using extracts from various plant parts like roots, leaves, and stems of plants such as *Hibiscus cannabinus* L, *Dracaena Cochinchinensis*, *Eucommia ulmoides*, *Allium sativum* extract, *Gloriosa superba*, *Fagonia cretica*, *Premna integrifolia* L, Seeds of *W. coagulans, Sargassum polycystum*, *Dillenia indica* L, *Brophyllum pinnatum* leave and investigated the antimicrobial activities of plant extract mediated AgNPs [14,25,38–42]. These natural sources contain bioactive compounds within their extracts that can effectively reduce metal ions to atoms, initiating nuclei formation of antimicrobial properties containing nanomaterial [39,40].

In various tropical and subtropical areas, banana fruits are extensively grown and cultivated, resulting in a global production of approximately 1.16×10^{8} metric tons by the year 2019 [43]. Following harvesting, many wastes are discarded despite their high interest due to their lignin, hemicellulose, and cellulose fraction concentration. These fractions have uses in a variety of sectors, including paper, food, and cosmetics. In addition to reducing pollution and environmental issues, farmers, especially those in relatively low-income areas, would benefit economically from the correct usage of banana waste [43].

This report examined the potential uses of green banana pulp extract as a bio-reducing agent and in developing low-cost, renewable electrical devices. Here, PE has been used (a) to synthesize the AgNPs, and (b) as an electrolyte solution for electrochemical cells instead of a chemical electrolyte. In such cells, biosynthesized AgNPs serve as catalysts that facilitate electron transfer from organic or inorganic compounds to an electrode, ultimately producing electricity [44]. This improvement was achieved by increasing the open circuit voltage (Voc), and short circuit current (Isc), while lowering the internal resistance, and voltage regulation of the cell.

Additionally, the antibacterial activities of PE-mediated AgNPs were evaluated against both gram-negative and gram-positive bacteria. The aim of this report is to the biosynthesis of AgNPs by using a new bio-reducing agent with considerable electrolytic as well as antibacterial activities.

2. Materials & methods

2.1. Collection of the banana and chemicals

The banana pulp extract (PE) used in the experiments was prepared from fresh bananas which were obtained from Jhenaidah, Bangladesh. The silver nitrate ($AgNO_3$) used in the experiments was brought from Sigma-Aldrich Chemicals. All experiments were conducted by using pure deionized (DI) water.

2.2. Preparation of the pulp extract

Fresh bananas were cleaned and peeled. 20 g of pulp were cooked for an hour at 50 °C with 100 ml of DI water while being stirred with a heated magnetic stirrer. The mixture was then cooled and filtered twice by using whatman filter papers 41 & 42 to eliminate the impurities. Eventually, the pulp extract was stored at 4 °C until further use.

2.3. Biosynthesis of AgNPs by using the pulp extract

Fig. 1 shows the schematic diagram of the biosynthesis of AgNPs and the color alterations that occur during the bio-reduction

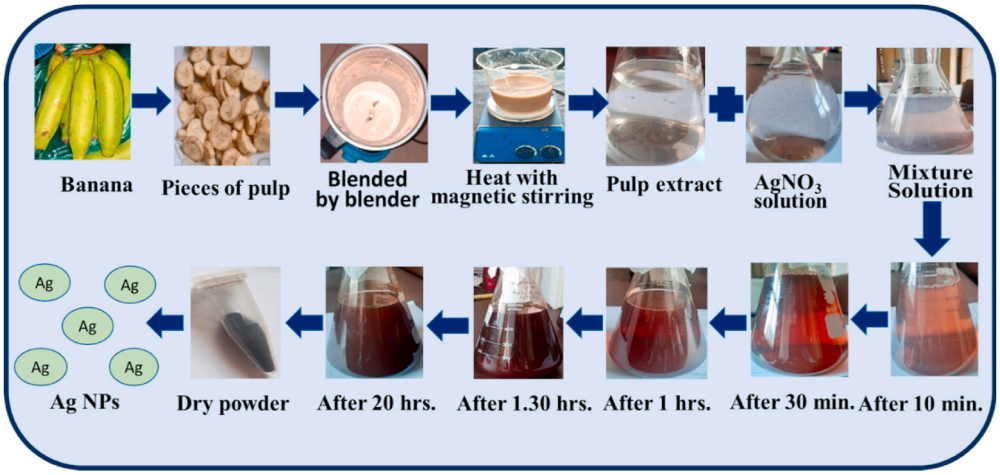

Fig. 1. Schematic diagram of biosynthesis of silver nanoparticles by using green banana pulp extract.

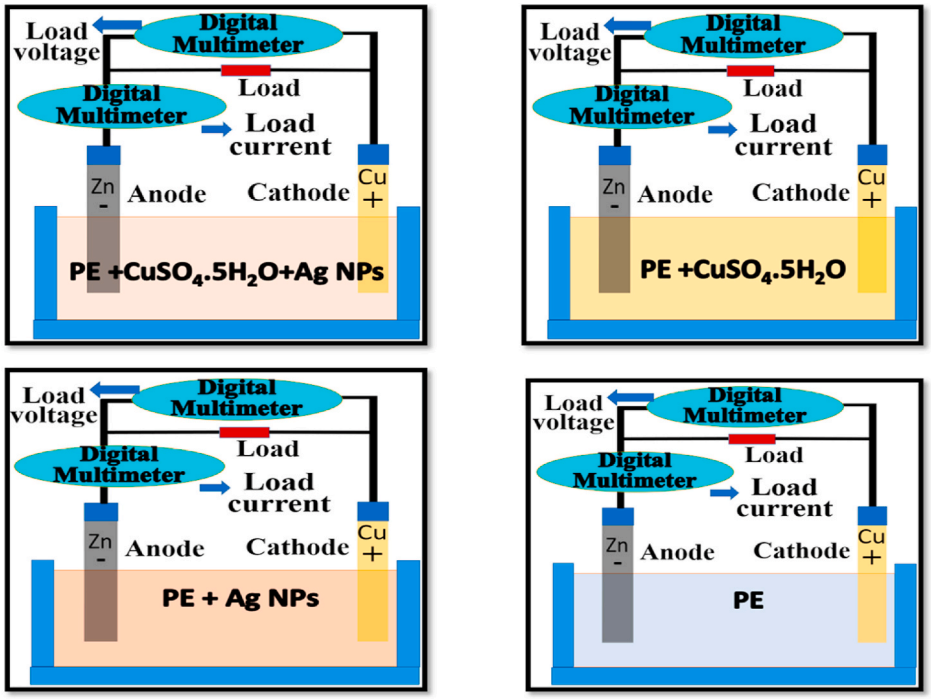

Fig. 2. The experimental setup of Zn/Cu electrode-based bio-electrochemical cell with load circuit.

process. 5 mL of aqueous pulp extract (PE) was added to 45 mL of 0.005 M $AgNO_3$ solution to reduce the silver ions. The light brownish-colored mixture solution was stored in the dark chamber to avoid the photo effect during the bio-reduction and over time the color of the mixture solution turned into dark brown. The exposure of PE to $AgNO_3$ solution indicates the formation of AgNPs by changing the color over time. The possible reaction mechanism can be as follows.

Step 1. $AgNO_3 \rightarrow Ag^+ + NO_3^-$

Step 2. $Ag^+ + (bio - reducing\ agent) \rightarrow Ag^0 \rightarrow AgNP_s$

2.4. Characterizations

X-ray diffraction technology was used to investigate the crystalline phase of AgNPs (Model: Smart Lab SE, Rigaku Corporation, Japan) with a scanning speed of 10° min^{-1} and a tube current/voltage of 40 mA/40 kV, a CuKα radiation source ($\lambda = 1.54059$ Å) was

Table 1
The combination of electrolytes for four bio-electrochemical cells.

Name of Cell	Electrolyte solution for the bio-electrochemical cells
Cell-P	100 mL (PE) + 100 mL $CuSO_4.5H_2O$ (1.2 M) + 30 mL (3 mg AgNPs)
Cell-Q	100 mL (PE) + 100 mL $CuSO_4.5H_2O$ (1.2 M)
Cell-R	100 mL (PE) + 30 mL (3 mg AgNPs)
Cell-S	100 mL (PE)

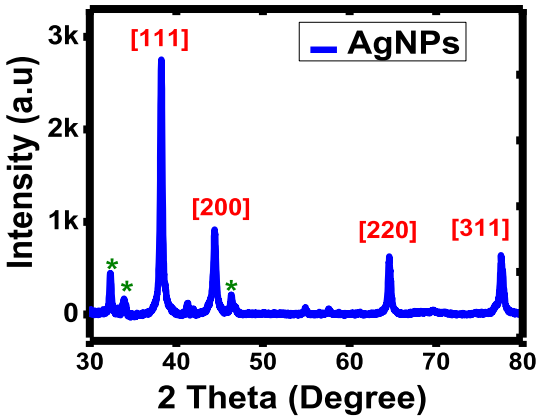

Fig. 3. XRD pattern of biosynthesized AgNPs.

used to record the diffraction pattern for biogenic AgNPs at ambient temperature. To examine the UV–visible spectrum between 200 and 1100 nm, a UV–Vis spectrophotometer (Model no: U-2900, Hitachi High-Tech Corporation, Tokyo, Japan) was utilized. To find functional groups in pulp extracts and AgNPs, FTIR spectrophotometry was carried out using a PerkinElmer (L1600300 Spectrum TWO LITA, UK) FT-IR spectrophotometer. The morphology of silver nanoparticles was studied with a JSM-7610 F-equipped apparatus for field emission scanning electron microscopy (FESEM). The AgNPs were coated for 10 s with an auto-fine platinum coater (JEC-3000FC) before taking images. The microstructures were examined utilizing the Thermoscientific Talos model transmission electron microscope (TEM). Gas chromatography-mass spectrometry analysis utilized a Clarus®690 gas chromatograph (PerkinElmer, CA, USA) with an Elite-35 column (30 m length, 0.25 mm diameter, 0.25 μm film thickness) and a Clarus® SQ 8 C mass spectrophotometer (PerkinElmer, CA, USA). Employing a 1 μL sample in split less mode, pure Helium (99.999 %) served as the carrier gas at a consistent flow rate (1 mL/min) over a 40-min runtime. Operating in EI mode at 70 eV, the inlet temperature remained constant at 280 °C while the column oven temperature started at 60 °C (0 min), ramping up at 5 °C per minute to 240 °C and holding for 4 min. Compound identification relied on comparison to the National Institute of Standards and Technology (NIST) database.

2.5. Antibacterial assay

The antimicrobial effectiveness of the newly produced AgNPs was gauged against gram negative *E. coli and* gram-positive *S. epidermidis* strains on Mueller-Hinton Agar using the disc diffusion method. The bacteria were sourced from the Microbiology Department at Jashore University of Science and Technology. The bacterial concentration was 1×10^8 CFU/ml, and the volume on each disc was 10 μl of extract solution for both concentrations. AgNPs (200 and 400 μg/disk) in wells were incubated at 37 °C, and inhibition zone diameters (mm) were measured after 24 h.

2.6. Designing of bio-electrochemical cell

Four distinct bio-electrochemical cells were used to examine the effects of AgNPs on the power-generating system. The design of the bio-electrochemical cells is shown in Fig. 2. Table 1 presents the mixture of bio-electrolytes for each cell. In this experiment, Zn and Cu plates with similar surface areas were selected as electrodes in Cell-P, Cell-Q, Cell-R, and Cell-S.

3. Result and discussions

3.1. X-ray diffraction analysis

Fig. 3 shows the X-ray diffraction pattern of biosynthesized AgNPs by using banana pulp extract. Four significant diffraction peaks at angle (2 theta) 38.19°, 44.39°, 64.58°, and 77.57° demonstrated the FCC structure of AgNPs with (111), (200), (220), and (311) planes respectively [45,46]. The results agreed well with the Joint Committee on Powder Diffraction Standards' database (JCPDS No:

Table 2
Crystallite size, interplanar spacing, and lattice parameters measurements for synthesized silver nanoparticles.

2θ of the intense peak (°)	FWHM β (°)	Miller indices (*hkl*)	Crystallite Diameter, D (nm)	Interplanar spacing, d (nm)	Lattice parameters, a (nm)
38.23	0.246	111	34.051	0.23	0.4075
44.39	0.344	200	24.92	0.21	0.4077
64.55	0.274	220	34.27	0.15	0.4079
77.51	0.320	311	31.80	0.13	0.4080

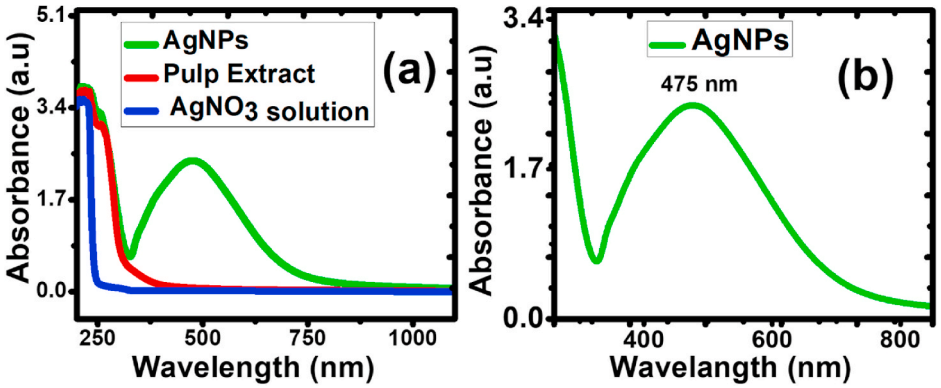

Fig. 4. UV–Vis spectra of (a) AgNPs (green line), Pulp Extract (red line), $AgNO_3$ (blue line), and (b) AgNPs.

65–2871) [3,8,47]. Few weak peaks (*) are appeared in the XRD spectra which may be attributed due to the bio-compounds of the extract on the surface of AgNPs [48,49]. The Debye-Scherrer equation, expressed in Eq.(*i*)

$$D = \frac{K\lambda}{\beta\, Cos\, \theta} - - - - \quad \text{(i)}$$

where λ represents the wavelength of X-rays, θ is the angle of Bragg's diffraction, and β represents the full width at half maximum (FWHM) [11,50–52]. The average crystal size of AgNPs was calculated to be 31.26 nm by using the Debye-Scherrer equation.

Additionally, Eq. (*ii*),

$$\frac{1}{d^2} = \frac{h^2 + k^2 + l^2}{a^2} - - - - \quad \text{(ii)}$$

along with Miller indices (hkl) of the planes, helps to determine the lattice constant [53]. For specific peaks detailed in Table 2, the calculated average lattice parameter was found to be about 0.4078 nm. This closely matches the known lattice parameter of silver nanoparticles in the JCPDS file (04–0783), which is 0.4086 nm [53,54].

Dislocations have a notable impact on material characteristics by distorting the regular atomic arrangement. The presence of structural defects in morphology, crystalline size, and the process of crystallite formation creates the dislocations. The quantification of these dislocations can be achieved using the Williamson-Smallman equation which is shown in Eq. (*iii*) that offers a convenient means of estimating the dislocation density (δ) [55]. The equation is given as:

$$\delta = \frac{1}{D^2} - - - - \quad \text{(iii)}$$

In this equation, the average crystal size, D, is determined to be 31.26 nm. Notably, a very low dislocation density value of 0.000055499 lines per nm^2 was found, indicating the high degree of crystallinity in the synthesized silver nanoparticles.

3.2. UV–vis absorption spectrophotometry analysis

Fig. 4 (a,b) represents the UV–visible spectra of bio-synthesized AgNPs. The highest absorbance of AgNPs occurred between 400 and 500 nm which indicates the presence of surface plasmon resonance (SPR) [56,57]. The maximum absorbance of bio-synthesized AgNPs was observed at a wavelength of 475 nm which may depend on the particle size, shape, and the type of reducing agents [57]. Following the addition of pulp extract to the $AgNO_3$ solution, the color shift of the mixture solution indicates the bio-reduction of Ag^+ to Ag^0 Hence, the reducing agents in the pulp extract played a crucial role in the formation of AgNPs.

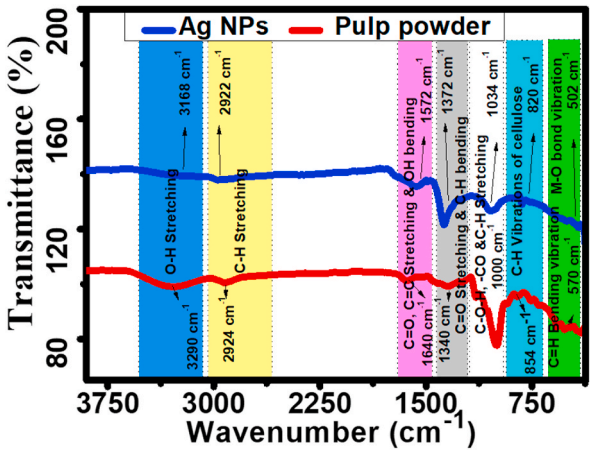

Fig. 5. FTIR spectra of pulp powder (red line), and AgNPs (blue line).

Table 3
Summary of FTIR analysis of pulp powder and pulp extract mediated AgNPs.

Functional groups	Wavenumber, n (cm^{-1})		
	Pulp powder	**AgNPs**	**Ref. value**
-OH stretching vibration of hydroxyl groups	3290	3168	3298 [57], 3396.12 [59]
stretching bands of the C–H bond & narrowing vibration of the HC groups	2924	2922	2927 [61]
C═O, C═C stretching vibration & broad OH bending	1640	1572	1651 [61], 1645 [62]
aliphatic C–H groups of bending bands, C–O stretching vibration of pyran typical of flavonoid	1340	1372	1371 [61],1343 [63]
C–*O*–H, –C═O stretching vibration & aromatic C–H stretching vibration	1000	1034	1003 [61],1032 [67]
C–H vibrations of cellulose	854	820	895 [62]
C═H bending vibration, Ag–O bonds	570	502	591 [57]

3.3. FTIR analysis

The FTIR analysis identifies active functional groups in the plant extract that are responsible for the bio-reduction of nanoparticles during the reaction mechanism. The presence of flavonoids and other phenolic compounds in the extract may cause the reduction of metal ions and the creation of the corresponding metal nanoparticles [57]. Fig. 5 represents the FTIR spectra of pulp power and the biosynthesized AgNPs. FTIR spectra of pulp extract revealed peaks at 3290, 2924, 1640, 1340, 1000, 854, and 570 cm^{-1} for the presence of different functional groups, which can play a significant role in the biosynthesis of metal or semiconductor oxide nanoparticles. The stretching of the hydroxyl group (-OH) from phenols and alcohols is responsible for the peak at wave number 3290 cm^{-1} [58–60]. The stretching and narrowing vibration of the C–H group corresponds to the peak at 2924 cm^{-1} [61]. Three prominent peaks at 1640 cm^{-1} are associated with C═O, C═C stretching bands, at 1340 for C–H bending of aliphatic, C–O stretching of flavonoids, at 1000 cm^{-1} is for C–*O*–H, –C═O and C–H stretching bands of aromatic groups [61–64]. In addition, the FTIR spectra revealed characteristic C–H vibrations of cellulose at 854 cm^{-1} [62]. These peaks are mainly responsible for the bio-reduction of metal nanoparticles by the plant extract reducing agents [65,66].

The FT-IR spectra of PE-mediated AgNPs showed changes in vibration frequencies from 3290, 2924, 1640, 1340, and 1000 cm^{-1} to 3168, 2922, 1572, 1372, and 1034 cm^{-1}. These changes suggest that silver ions were reduced and that newly formed silver nanoparticles were capped as well as stabilized through interactions with biomolecules such as alcohols, terpenes, tannins, phenols, and terpenoids in the pulp extract [58,61]. Table 3 represents the detailed analysis of the corresponding functional groups in pulp extract and AgNPs.

3.4. Gas chromatography-mass spectrometry analysis

The constituents of the green banana pulp extract were analyzed by the GC-MS analysis. GC-MS analysis of PE identified 12 compounds. Fig. 6 displays the distinctive chromatogram. Table 4 showcases bioactive compounds from PE, detailing their retention times (RT), identified compounds, molecular weights, and peak areas (%). Predominantly, 1,4-di-o-acetyl-2,3,5-tri-*o*-methylribitol (1.09 %), Methyl 13-phenyl-tridecanoate (1.52 %), 1-methyl-1-ethoxycyclobutane (0.96 %), and Naphthalene, 1,2,3,4-tetrahydro-1,4-dimethyl (0.82 %) were the major components found in the extract based on their abundance.

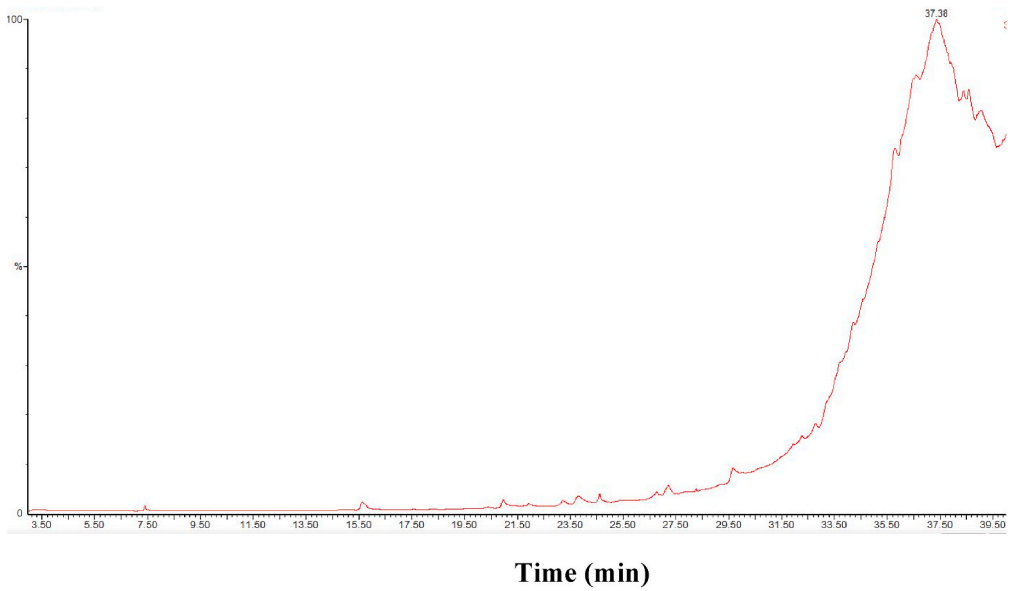

Fig. 6. GCMS chromatogram of ethanol extract of green banana pulp extract.

Table 4
GC-MS analysis of green banana pulp extract.

Serial No.	Retention time (RT)	Identified compounds	Molecular weight	Peak area (%)
1	7.40	Hexadecane	226	0.29
2	15.63	1-methyl-1-ethoxycyclobutane	114	0.96
3	20.96	Naphthalene, 1,2,3,4-tetrahydro-1,4-dimethyl	160	0.82
4	21.93	2,2,4-trimethyl-1,3-pentanediol diisobutyrate	286	0.26
5	23.23	Coronarin E	284	0.42
6	23.82	1,4-di-o-acetyl-2,3,5-tri-*o*-methylribitol	278	1.09
7	24.62	Diethyl phthalate	222	0.47
8	27.22	N-hexadecanoic acid	256	0.82
9	28.26	Tetradecanoic acid, 10,13-dimethyl-, methyl ester	270	0.05
10	32.26	I-propyl 5,9,19-octacosatrienoate	460	0.02
11	32.79	Methyl 5,13-docosadienoate	350	0.36
12	35.79	Methyl 13-phenyl-tridecanoate	304	1.52

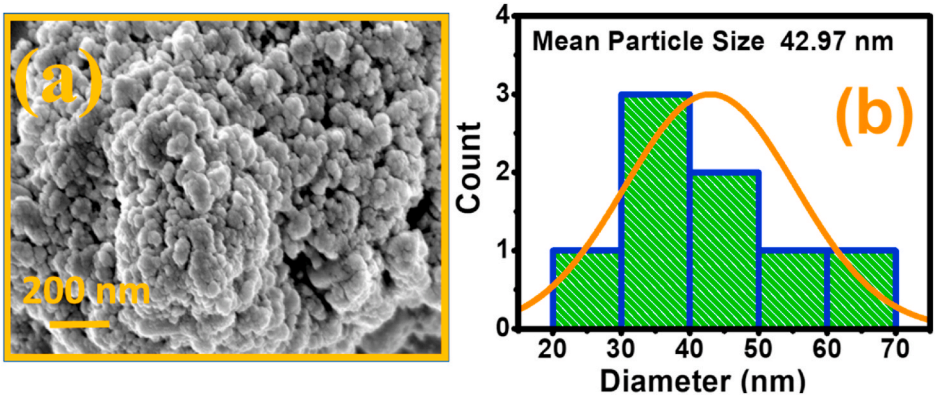

Fig. 7. (a) FESEM images of AgNPs and (b) mean particle size histogram of AgNPs.

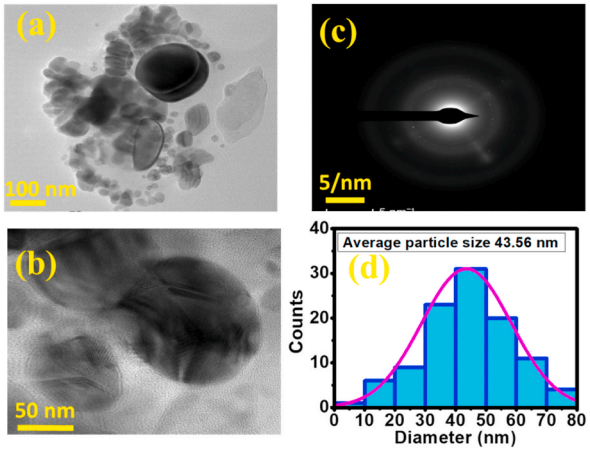

Fig. 8. TEM image of AgNPs in different scales (a) 100 nm, (b) 50 nm, and (c) SAED pattern of silver nanoparticles, (d) particle size histogram.

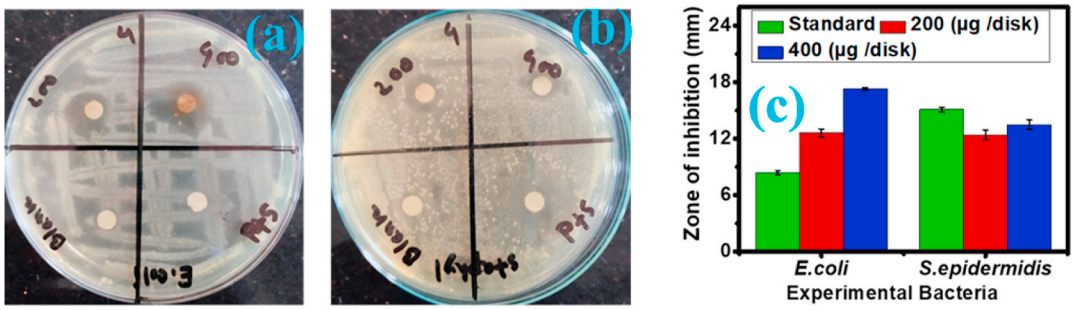

Fig. 9. Illustrates the inhibition zone size of AgNPs and control ethanol for *E. coli* and *S. epidermidis,* including images (a), (b) and bar graphs (c).

3.5. Morphology analysis of AgNPs

Plant extracts can be used to adjust the concentrations and rates of reducing, capping, and stabilizing agents, thereby altering the shape and size of metallic nanoparticles [54,68]. Fig. 7 (a) represents the high-resolution image of silver nanoparticles obtained through FESEM imaging at a scale of 200 nm. The image shows almost spherical particle sizes of biosynthesized AgNPs. The size distribution of silver nanoparticles was determined by using Image J software analysis shown in Fig. 7 (b), ranging from 20 nm to 70 nm. The average size of the particles is found to be 42.97 nm.

3.6. TEM analysis of AgNPs

TEM was employed to capture high-resolution images of AgNPs created through green banana pulp extract (GBPE). Fig. 8(a–d) reveals the TEM analysis of spherical AgNPs. Detailed views show a transparent layer on their surfaces, likely resulting from biomolecules in GBPE. This extract acted as both a reducer and a capping agent, preventing excessive aggregation and ensuring stability. Particle size averaged 43.56 nm, consistent with FESEM findings 42.97 nm.

4. Antibacterial activity of green banana pulp extract synthesized AgNPs

The antibacterial activities of green banana pulp extract-mediated AgNPs have been evaluated at different concentrations (200 and 400 µg/disk) against two pathogenic bacteria: *E. coli* (gram-negative*)* and *S. epidermidis* (gram-positive). The disc diffusion method was employed where ethanol was used as a control. Generally, the diameter of the zone of inhibition was measured which indicates the antimicrobial activity of the NPs [69,70]. Fig. 9(a–c) shows that AgNPs exhibited significant antibacterial effects against both gram-negative and gram-positive bacteria at both concentrations after 24 h of incubation at 37 °C. The inhibition zone increased as the concentration of AgNPs increased. Interestingly, the *E. coli* bacteria had a greater inhibitory zone than the *S. epidermidis* bacteria, which was consistent with the NPs also. The size of the inhibition zone for each bacterial strain and the mean values are shown in Table 5 with statistical analysis. The assessment compared the antibacterial efficacy of standard antibiotics and AgNPs at different concentrations against both gram-negative and gram-positive bacteria. For *E. coli,* AgNPs displayed a dose-dependent increase in inhibition zones (12.6 ± 0.42 mm and 17.3 ± 0.14 mm at 200 µg/disk and 400 µg/disk, respectively), while the standard antibiotic showed an 8.4 ±

Table 5
Antibacterial activity of the AgNPs.

Bacterial strain	Inhibition zone (mm)		
	Standard antibiotic (Azithromycin) (mm)	AgNPs (n = 2 replicates per concentration)	
		200 μg/disk	400 μg/disk
Escherichia coli	8.4 ± 0.21	12.6 ± 0.42	17.3 ± 0.14
Staphylococcus epidermidis	15.1 ± 0.28	12.4 ± 0.49	13.5 ± 0.49

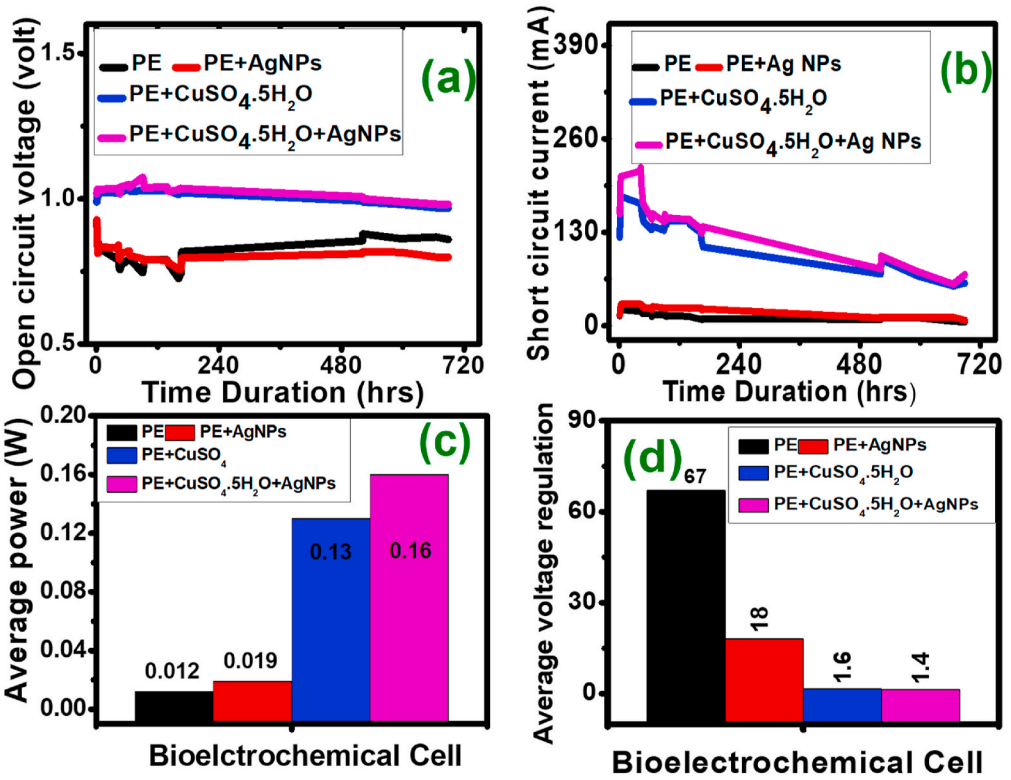

Fig. 10. Displays the electrical activity of cells for (a) open circuit voltage, (b) short circuit current (c) power, and (d) voltage regulation for 5Ω load resistance.

0.21 mm zone. Similarly, against *S. epidermidis*, AgNPs presented zones of 12.4 ± 0.49 mm and 13.5 ± 0.49 mm at the respective concentrations, whereas the standard antibiotic had a 15.1 ± 0.28 mm zone. This highlights the distinct impact of AgNPs on bacterial growth without focusing on their combined or synergestic effects. These findings demonstrate the promising antimicrobial potential of biosynthesized AgNPs against pathogenic bacteria.

The inhibition zones (in millimeters) against *E. coli* and *S. epidermidis* resulting from varying concentrations of AgNPs compared to a standard antibiotic treatment. Error bars represent mean ± standard deviation (n = 2 replicates per concentration). The blue bars represent the effect of AgNPs (400 μg/disk) on both bacterial strains, while the red bars depict the impact of AgNPs (200 μg/disk). The green bars signify the standard antibiotic. Although standard deviations are provided, the figure lacks corresponding standard errors, preventing a detailed explanation of significance levels or statistical analysis. This comprehensive legend clarifies the figure's content, color associations, and the significance of different bar colors in comparing the data. Here, Azithromycin antibiotic was taken as standard antibiotic and the disc concentration of 6 mg/ml was used during the experiment.

5. Electrical activities of biosynthesized AgNPs

This study aimed to examine the impact of AgNPs on power generation in bio-electrochemical cells. Four cells were created using different bio-electrolyte solutions and their electrical performances were monitored over time. Fig. 10(a–d) revealed that all cells can generate electricity using plant extract electrolytes. However, the cell with AgNPs (Cell-P) demonstrated significantly higher open circuit voltage and short circuit current compared to the other cells. Consequently, Cell-P had the highest maximum power output and the lowest internal resistance among the four cells. The maximum power output of Cell-P was calculated to be 0.16 W, while Cell-S had

Table 6
Electrical properties of bio electrochemical cells in the absence of load resistance.

Name of the cell	Average open circuit voltage (volt)	Average short circuit current (A)	Average power (watt)	Average voltage regulation for 5Ω load resistance
Cell-P	1.02916	0.15355	0.15849	1.40
Cell-Q	1.01466	0.13507	0.13748	1.60
Cell-R	0.80769	0.0231	0.01864	18.00
Cell-S	0.80219	0.01446	0.01159	67.00

the lowest power output of 0.012 W. The average electrical performances of Cells P, Q, R, and S were compared in Table 6. Overall, the findings suggest that the incorporation of AgNPs in bio-electrochemical cells can enhance their power generation capabilities. In addition, 5 Ω load resistance were connected to all cells and the voltage regulations were measured. Among the four cells, Cell-P, which utilized $CuSO_4.5H_2O$ and AgNPs with pulp extract electrolyte solution had the lowest value of voltage regulation at 1.40.

6. Conclusions

The utilization of green resources for synthesizing silver nanoparticles presents a superior alternative to chemical methods due to its eco-friendly and cost-effective nature. We developed a rapid, eco-friendly method for synthesizing AgNPs using green banana pulp extract, devoid of chemical solvents. The resulting AgNPs exhibited potent antibacterial activity against both gram-negative and gram-positive bacteria, with inhibition zones increasing with higher concentrations. Notably, *E. coli* displayed a larger inhibitory zone compared to *S. epidermidis*, underscoring the efficacy against these pathogens. This study investigated the impact of various factors such as current, voltage, power generation, voltage regulation of pulp extract-based electrochemical cells over time and changes in load resistance. Remarkably, voltage and current increased as internal resistance decreased, and voltage regulation improved upon adding AgNPs to BEC. The AgNPs-based bio-electrochemical cell (Cell-P) demonstrated superior average power and voltage, attributed to its low voltage regulation and extended lifespan compared to other cell types. Ultimately, this research introduces a novel application of green banana pulp extract and AgNPs in bio-electrochemical cells, holding potential for sustainable and eco-friendly energy production. The utilization of green banana pulp extract for synthesizing silver nanoparticles showcases a promising avenue for sustainable antibacterial applications and enhanced bio-electrochemical cell performance, emphasizing the potential of eco-friendly approaches in advancing both healthcare and renewable energy technologies.

CRediT authorship contribution statement

Md Ohiduzzaman: Writing – original draft, Visualization, Methodology, Investigation, Funding acquisition, Formal analysis, Data curation, Conceptualization. **M.N.I. Khan:** Writing – review & editing, Supervision. **K.A. Khan:** Writing – review & editing, Supervision, Funding acquisition, Conceptualization. **Bithi Paul:** Writing – review & editing, Validation, Investigation, Formal analysis, Conceptualization.

Declaration of competing interest

The authors declare the following financial interests/personal relationships which may be considered as potential competing interests:Md Ohiduzzaman reports financial support was provided by Government of the People's Republic of Bangladesh Ministry of Science and Technology. If there are other authors, they declare that they have no known competing financial interests or personal relationships that could have appeared to influence the work reported in this paper.

Acknowledgments

This work is supported by the NST (National Science and Technology) Fellowship, Ministry of Science and Technology, Government of Bangladesh (GoB) (Award Id: 120005100-3821117). The authors would like to acknowledge the Atomic Energy Centre, Dhaka, and Jashore University of Science and Technology, Jashore-7408, Bangladesh to provide the required facilities during this research.

References

[1] S. Kumar, et al., Plant extract mediated silver nanoparticles and their applications as antimicrobials and in sustainable food packaging: a state-of-the-art review, Trends Food Sci. Technol. 112 (Jun. 2021) 651–666, https://doi.org/10.1016/j.tifs.2021.04.031.

[2] K.C. Hembram, R. Kumar, L. Kandha, P.K. Parhi, C.N. Kundu, B.K. Bindhani, Therapeutic prospective of plant-induced silver nanoparticles: application as antimicrobial and anticancer agent, Artif. Cell Nanomed. Biotechnol. 46 (sup3) (Nov. 2018) 38–51. Green synthesis of Ag nanoparticles using Tamarind fruit extract for the antibacterial studies.

[3] N. Jayaprakash, et al., Green synthesis of Ag nanoparticles using Tamarind fruit extract for the antibacterial studies, J. Photochem. Photobiol. B Biol. 169 (Apr. 2017) 178–185, https://doi.org/10.1016/j.jphotobiol.2017.03.013.

[4] P. Banerjee, M. Satapathy, A. Mukhopahayay, P. Das, Leaf extract mediated green synthesis of silver nanoparticles from widely available Indian plants: synthesis, characterization, antimicrobial property and toxicity analysis, Bioresour. Bioprocess. 1 (1) (Dec. 2014) 3, https://doi.org/10.1186/s40643-014-0003-y.

[5] V. Gopinath, D. MubarakAli, S. Priyadarshini, N.M. Priyadharsshini, N. Thajuddin, P. Velusamy, Biosynthesis of silver nanoparticles from Tribulus terrestris and its antimicrobial activity: a novel biological approach, Colloids Surf. B Biointerfaces 96 (Aug. 2012) 69–74, https://doi.org/10.1016/j.colsurfb.2012.03.023.

[6] S. Faisal, et al., Green synthesis of zinc oxide (ZnO) nanoparticles using aqueous fruit extracts of *Myristica fragrans* : their Characterizations and biological and environmental applications, ACS Omega 6 (14) (Apr. 2021) 9709–9722, https://doi.org/10.1021/acsomega.1c00310.

[7] M. Darroudi, M. Mansor Bin Ahmad, A.H. Abdullah, N.A. Ibrahim, K. Shameli, Green synthesis and characterization of gelatin-based and sugar-reduced silver nanoparticles, IJN (Mar. 2011) 569, https://doi.org/10.2147/IJN.S16867.

[8] M. Shahriary, H. Veisi, M. Hekmati, S. Hemmati, In situ green synthesis of Ag nanoparticles on herbal tea extract (Stachys lavandulifolia)-modified magnetic iron oxide nanoparticles as antibacterial agent and their 4-nitrophenol catalytic reduction activity, Mater. Sci. Eng. C 90 (Sep. 2018) 57–66, https://doi.org/10.1016/j.msec.2018.04.044.

[9] S. Hamedi, S.A. Shojaosadati, A. Mohammadi, Evaluation of the catalytic, antibacterial and anti-biofilm activities of the Convolvulus arvensis extract functionalized silver nanoparticles, J. Photochem. Photobiol. B Biol. 167 (Feb. 2017) 36–44, https://doi.org/10.1016/j.jphotobiol.2016.12.025.

[10] P.K. Jain, X. Huang, I.H. El-Sayed, M.A. El-Sayed, Noble metals on the nanoscale: optical and photothermal properties and some applications in imaging, sensing, biology, and medicine, Acc. Chem. Res. 41 (12) (Dec. 2008) 1578–1586, https://doi.org/10.1021/ar7002804.

[11] V. Selvaraj, S. Sagadevan, L. Muthukrishnan, Mohd R. Johan, J. Podder, Eco-friendly approach in synthesis of silver nanoparticles and evaluation of optical, surface morphological and antimicrobial properties, J Nanostruct Chem 9 (2) (Jun. 2019) 153–162, https://doi.org/10.1007/s40097-019-0306-9.

[12] K. Anandalakshmi, J. Venugobal, V. Ramasamy, Characterization of silver nanoparticles by green synthesis method using Pedalium murex leaf extract and their antibacterial activity, Appl. Nanosci. 6 (3) (Mar. 2016) 399–408. Characterization and evaluation of cytotoxic and apoptotic effects of green synthesis of silver nanoparticles using Artemisia Ciniformis on human gastric adenocarcinoma.

[13] N. Hashim, et al., Green mode synthesis of silver nanoparticles using Vitis vinifera's tannin and screening its antimicrobial activity/apoptotic potential versus cancer cells, Mater. Today Commun. 25 (Dec. 2020) 101511, https://doi.org/10.1016/j.mtcomm.2020.101511.

[14] M. Ohiduzzaman, M.N.I. Khan, K.A. Khan, B. Paul, Green synthesis of silver nanoparticles by using Allium sativum extract and evaluation of their electrical activities in bio-electrochemical cell, Nanotechnology 35 (9) (Feb. 2024) 095707, https://doi.org/10.1088/1361-6528/ad10e4.

[15] G. Li, et al., Fungus-mediated green synthesis of silver nanoparticles using Aspergillus terreus, IJMS 13 (1) (Dec. 2011) 466–476, https://doi.org/10.3390/ijms13010466.

[16] D. MubarakAli, N. Thajuddin, K. Jeganathan, M. Gunasekaran, Plant extract mediated synthesis of silver and gold nanoparticles and its antibacterial activity against clinically isolated pathogens, Colloids Surf. B Biointerfaces 85 (2) (Jul. 2011) 360–365, https://doi.org/10.1016/j.colsurfb.2011.03.009.

[17] T.C. Prathna, N. Chandrasekaran, A.M. Raichur, A. Mukherjee, Biomimetic synthesis of silver nanoparticles by Citrus limon (lemon) aqueous extract and theoretical prediction of particle size, Colloids Surf. B Biointerfaces 82 (1) (Jan. 2011) 152–159, https://doi.org/10.1016/j.colsurfb.2010.08.036.

[18] B. Subhasree, R. Baskar, R. Laxmi Keerthana, R. Lijina Susan, P. Rajasekaran, Evaluation of antioxidant potential in selected green leafy vegetables, Food Chem. 115 (4) (Aug. 2009) 1213–1220, https://doi.org/10.1016/j.foodchem.2009.01.029.

[19] A. Bankar, B. Joshi, A.R. Kumar, S. Zinjarde, Banana peel extract mediated novel route for the synthesis of silver nanoparticles, Colloids Surf. A Physicochem. Eng. Asp. 368 (1–3) (Sep. 2010) 58–63, https://doi.org/10.1016/j.colsurfa.2010.07.024.

[20] A. Nabikhan, K. Kandasamy, A. Raj, N.M. Alikunhi, Synthesis of antimicrobial silver nanoparticles by callus and leaf extracts from saltmarsh plant, Sesuvium portulacastrum L, Colloids Surf. B Biointerfaces 79 (2) (Sep. 2010) 488–493, https://doi.org/10.1016/j.colsurfb.2010.05.018.

[21] V. Dhand, L. Soumya, S. Bharadwaj, S. Chakra, D. Bhatt, B. Sreedhar, Green synthesis of silver nanoparticles using Coffea arabica seed extract and its antibacterial activity, Mater. Sci. Eng. C 58 (Jan. 2016) 36–43, https://doi.org/10.1016/j.msec.2015.08.018.

[22] G.L. Vanti, et al., Synthesis of *Gossypium hirsutum* -derived silver nanoparticles and their antibacterial efficacy against plant pathogens, Appl. Organomet. Chem. 33 (1) (Jan. 2019) e4630, https://doi.org/10.1002/aoc.4630.

[23] B. Nandini, H. Puttaswamy, H.S. Prakash, S. Adhikari, S. Jogaiah, G. Nagaraja, Elicitation of novel trichogenic-lipid nanoemulsion signaling resistance against pearl millet downy mildew disease, Biomolecules 10 (1) (Dec. 2019) 25, https://doi.org/10.3390/biom10010025.

[24] J. Sangeetha, et al., in: R. Prasad Nanotechnology, M. Kumar, V. Kumar (Eds.), Production of Bionanomaterials from Agricultural Wastes, Springer Singapore, Singapore, 2017, pp. 33–58, https://doi.org/10.1007/978-981-10-4573-8_3.

[25] S. Nayak, M.P. Bhat, A.C. Udayashankar, T.R. Lakshmeesha, N. Geetha, S. Jogaiah, Biosynthesis and characterization of *Dillenia indica* -mediated silver nanoparticles and their biological activity, Appl. Organomet. Chem. 34 (4) (Apr. 2020) e5567, https://doi.org/10.1002/aoc.5567.

[26] V. Kumar, S.K. Yadav, Plant-mediated synthesis of silver and gold nanoparticles and their applications, J. Chem. Technol. Biotechnol. 84 (2) (Feb. 2009) 151–157, https://doi.org/10.1002/jctb.2023.

[27] K.S. Mukunthan, S. Balaji, Cashew apple juice (*Anacardium occidentale* L.) speeds up the synthesis of silver nanoparticles, Int. J. Green Nanotechnol. 4 (2) (Apr. 2012) 71–79, https://doi.org/10.1080/19430892.2012.676900.

[28] P. Nartop, Effects of surface sterilisation with green synthesised silver nanoparticles on Lamiaceae seeds, IET Nanobiotechnol. 12 (5) (Aug. 2018) 663–668, https://doi.org/10.1049/iet-nbt.2017.0195.

[29] S. Jogaiah, M. Kurjogi, M. Abdelrahman, N. Hanumanthappa, L.-S.P. Tran, Ganoderma applanatum-mediated green synthesis of silver nanoparticles: structural characterization, and in vitro and in vivo biomedical and agrochemical properties, Arab. J. Chem. 12 (7) (Nov. 2019) 1108–1120, https://doi.org/10.1016/j.arabjc.2017.12.002.

[30] M. Hasan, et al., Mechanistic study of silver nanoparticle's synthesis by dragon's blood resin ethanol extract and antiradiation activity, j nanosci nanotechnol 15 (2) (Feb. 2015) 1320–1326, https://doi.org/10.1166/jnn.2015.9090.

[31] M.S. Saif, et al., Phyto-reflexive Zinc Oxide Nano-Flowers synthesis: an advanced photocatalytic degradation and infectious therapy, J. Mater. Res. Technol. 13 (Jul. 2021) 2375–2391, https://doi.org/10.1016/j.jmrt.2021.05.107.

[32] E. Elemike, O. Fayemi, A. Ekennia, D. Onwudiwe, E. Ebenso, Silver nanoparticles mediated by Costus afer leaf extract: synthesis, antibacterial, antioxidant and electrochemical properties, Molecules 22 (5) (Apr. 2017) 701, https://doi.org/10.3390/molecules22050701.

[33] H. Ahmad, et al., Green synthesis and characterization of zinc oxide nanoparticles using Eucalyptus globules and their fungicidal ability against pathogenic fungi of apple orchards, Biomolecules 10 (3) (Mar. 2020) 425, https://doi.org/10.3390/biom10030425.

[34] H. Ji, et al., Size-controllable preparation and antibacterial mechanism of thermo-responsive copolymer-stabilized silver nanoparticles with high antimicrobial activity, Mater. Sci. Eng. C 110 (May 2020) 110735, https://doi.org/10.1016/j.msec.2020.110735.

[35] D. Chen, X. Li, T. Soule, F. Yorio, L. Orr, Effects of solution chemistry on antimicrobial activities of silver nanoparticles against Gordonia sp, Sci. Total Environ. 566 (567) (Oct. 2016) 360–367, https://doi.org/10.1016/j.scitotenv.2016.05.037.

[36] N. Konappa, et al., Ameliorated antibacterial and antioxidant properties by Trichoderma harzianum mediated green synthesis of silver nanoparticles, Biomolecules 11 (4) (Apr. 2021) 535, https://doi.org/10.3390/biom11040535.

[37] N. Durán, G. Nakazato, A.B. Seabra, Antimicrobial activity of biogenic silver nanoparticles, and silver chloride nanoparticles: an overview and comments, Appl. Microbiol. Biotechnol. 100 (15) (Aug. 2016) 6555–6570, https://doi.org/10.1007/s00253-016-7657-7.

[38] S.Y. Chew, S.Y. Teoh, Y.Y. Sim, K.L. Nyam, Optimization of ultrasonic extraction condition for maximal antioxidant, antimicrobial, and antityrosinase activity from Hibiscus cannabinus L. leaves by using the single factor experiment, Journal of Applied Research on Medicinal and Aromatic Plants 25 (Dec. 2021) 100321, https://doi.org/10.1016/j.jarmap.2021.100321.

[39] H. Zulfiqar, et al., Synthesis of silver nanoparticles using *Fagonia cretica* and their antimicrobial activities, Nanoscale Adv. 1 (5) (2019) 1707–1713, https://doi.org/10.1039/C8NA00343B.

[40] M. Hasan, et al., Assessment of bioreducing and stabilizing potential of dragon's blood (Dracaena Cochinchinensis, lour. S. C. Chen) resin extract in synthesis of silver nanoparticles, Nanosci. Nanotechnol. Lett. 5 (7) (Jul. 2013) 780–784, https://doi.org/10.1166/nnl.2013.1600.

[41] M. Hasan, et al., Bioinspired synthesis of zinc oxide nano-flowers: a surface enhanced antibacterial and harvesting efficiency, Mater. Sci. Eng. C 119 (Feb. 2021) 111280, https://doi.org/10.1016/j.msec.2020.111280.

[42] M.A. Hossain, B. Paul, K.A. Khan, M. Paul, M.A. Mamun, M.E. Quayum, Green synthesis and characterization of silver nanoparticles by using Bryophyllum pinnatum and the evaluation of its power generation activities on bio-electrochemical cell, Mater. Chem. Phys. 282 (Apr. 2022) 125943, https://doi.org/10.1016/j.matchemphys.2022.125943.
[43] G. Gardos, J.O. Cole, Maintenance antipsychotic therapy: is the cure worse than the disease? Am J Psychiatry 133 (1) (Jan. 1976) 32–36, https://doi.org/10.1176/ajp.133.1.32.
[44] R.G. Fiddian-Green, W. Silen, Mechanisms of disposal of acid and alkali in rabbit duodenum, Am. J. Physiol. 229 (6) (Dec. 1975) 1641–1648, https://doi.org/10.1152/ajplegacy.1975.229.6.1641.
[45] Th B. Devi, M. Ahmaruzzaman, Bio-inspired sustainable and green synthesis of plasmonic Ag/AgCl nanoparticles for enhanced degradation of organic compound from aqueous phase, Environ. Sci. Pollut. Res. 23 (17) (Sep. 2016) 17702–17714, https://doi.org/10.1007/s11356-016-6945-1.
[46] F. Göl, A. Aygün, A. Seyrankaya, T. Gür, C. Yenikaya, F. Şen, Green synthesis and characterization of Camellia sinensis mediated silver nanoparticles for antibacterial ceramic applications, Mater. Chem. Phys. 250 (Aug. 2020) 123037, https://doi.org/10.1016/j.matchemphys.2020.123037.
[47] S. Jebril, R. Khanfir Ben Jenana, C. Dridi, Green synthesis of silver nanoparticles using Melia azedarach leaf extract and their antifungal activities: in vitro and in vivo, Mater. Chem. Phys. 248 (Jul. 2020) 122898, https://doi.org/10.1016/j.matchemphys.2020.122898.
[48] P. Das, K. Ghosal, N.K. Jana, A. Mukherjee, P. Basak, Green synthesis and characterization of silver nanoparticles using belladonna mother tincture and its efficacy as a potential antibacterial and anti-inflammatory agent, Mater. Chem. Phys. 228 (Apr. 2019) 310–317, https://doi.org/10.1016/j.matchemphys.2019.02.064.
[49] M. Mosaviniya, T. Kikhavani, M. Tanzifi, M. Tavakkoli Yaraki, P. Tajbakhsh, A. Lajevardi, Facile green synthesis of silver nanoparticles using Crocus Haussknechtii Bois bulb extract: catalytic activity and antibacterial properties, Colloid and Interface Science Communications 33 (Nov. 2019) 100211, https://doi.org/10.1016/j.colcom.2019.100211.
[50] A.A. Kulkarni, B.M. Bhanage, Ag@AgCl nanomaterial synthesis using sugar cane juice and its application in degradation of azo dyes, ACS Sustainable Chem. Eng. 2 (4) (Apr. 2014) 1007–1013, https://doi.org/10.1021/sc4005668.
[51] B. Paul, A. Mamun, A. Haque, M. Paul, A. Zkria, K. Ghosh, Nano-bio effects: interaction of ZnO and DNA-bases, Nano-Structures & Nano-Objects 31 (Jul. 2022) 100898, https://doi.org/10.1016/j.nanoso.2022.100898.
[52] B. Paul, M.A.-A. Mamun, A. Haque, M. Paul, K. Ghosh, Significant reduction of defect states and surface tailoring in ZnO nanoparticles via nano-bio interaction with glucose for bio-applications, IEEE Trans.on Nanobioscience 18 (3) (Jul. 2019) 490–497, https://doi.org/10.1109/TNB.2019.2919231.
[53] R.F.N. Quadrado, G. Gohlke, R.S. Oliboni, A. Smaniotto, A.R. Fajardo, Hybrid hydrogels containing one-step biosynthesized silver nanoparticles: preparation, characterization and catalytic application, J. Ind. Eng. Chem. 79 (Nov. 2019) 326–337, https://doi.org/10.1016/j.jiec.2019.07.008.
[54] M. Zhou, Z. Wei, H. Qiao, L. Zhu, H. Yang, T. Xia, Particle size and pore structure characterization of silver nanoparticles prepared by confined arc plasma, J. Nanomater. 2009 (2009) 1–5, https://doi.org/10.1155/2009/968058.
[55] S.S. Gandhad, et al., Synthesis and characterization of silver nanoparticles using green route, International Journal of Advanced Science and Engineering 8 (3) (Feb. 2022) 2252, https://doi.org/10.29294/IJASE.8.3.2022.2252-2259.
[56] J.M. Ashraf, M.A. Ansari, H.M. Khan, M.A. Alzohairy, I. Choi, Green synthesis of silver nanoparticles and characterization of their inhibitory effects on AGEs formation using biophysical techniques, Sci. Rep. 6 (1) (Feb. 2016) 20414, https://doi.org/10.1038/srep20414.
[57] S. Pugazhendhi, E. Kirubha, P.K. Palanisamy, R. Gopalakrishnan, Synthesis and characterization of silver nanoparticles from Alpinia calcarata by Green approach and its applications in bactericidal and nonlinear optics, Appl. Surf. Sci. 357 (Dec. 2015) 1801–1808, https://doi.org/10.1016/j.apsusc.2015.09.237.
[58] T.Í.S. Oliveira, et al., Bionanocomposite films based on polysaccharides from banana peels, Int. J. Biol. Macromol. 101 (Aug. 2017) 1–8, https://doi.org/10.1016/j.ijbiomac.2017.03.068.
[59] T.S. Alomar, N. AlMasoud, M.A. Awad, M.F. El-Tohamy, D.A. Soliman, An eco-friendly plant-mediated synthesis of silver nanoparticles: characterization, pharmaceutical and biomedical applications, Mater. Chem. Phys. 249 (Jul. 2020) 123007, https://doi.org/10.1016/j.matchemphys.2020.123007.
[60] M.H. Kahsay, A. Tadesse, D. RamaDevi, N. Belachew, K. Basavaiah, Green synthesis of zinc oxide nanostructures and investigation of their photocatalytic and bactericidal applications, RSC Adv. 9 (63) (2019) 36967–36981, https://doi.org/10.1039/C9RA07630A.
[61] P.A. Méndez, Á.M. Méndez, L.N. Martínez, B. Vargas, B.L. López, Cassava and banana starch modified with maleic anhydride-poly (ethylene glycol) methyl ether (Ma-mPEG): a comparative study of their physicochemical properties as coatings, Int. J. Biol. Macromol. 205 (Apr. 2022) 1–14, https://doi.org/10.1016/j.ijbiomac.2022.02.053.
[62] J.A. García-Ramón, et al., Morphological, barrier, and mechanical properties of banana starch films reinforced with cellulose nanoparticles from plantain rachis, Int. J. Biol. Macromol. 187 (Sep. 2021) 35–42, https://doi.org/10.1016/j.ijbiomac.2021.07.112.
[63] X. Li, H. Jiang, Y. Pu, J. Cao, W. Jiang, Inhibitory effect of condensed tannins from banana pulp on cholesterol esterase and mechanisms of interaction, J. Agric. Food Chem. 67 (51) (Dec. 2019) 14066–14073, https://doi.org/10.1021/acs.jafc.9b05212.
[64] T.U. Doan Thi, T.T. Nguyen, Y.D. Thi, K.H. Ta Thi, B.T. Phan, K.N. Pham, Green synthesis of ZnO nanoparticles using orange fruit peel extract for antibacterial activities, RSC Adv. 10 (40) (2020) 23899–23907, https://doi.org/10.1039/D0RA04926C.
[65] L. Rastogi, J. Arunachalam, Sunlight based irradiation strategy for rapid green synthesis of highly stable silver nanoparticles using aqueous garlic (Allium sativum) extract and their antibacterial potential, Mater. Chem. Phys. 129 (1–2) (Sep. 2011) 558–563, https://doi.org/10.1016/j.matchemphys.2011.04.068.
[66] D. Jini, S. Sharmila, A. Anitha, M. Pandian, R.M.H. Rajapaksha, In vitro and in silico studies of silver nanoparticles (AgNPs) from Allium sativum against diabetes, Sci. Rep. 12 (1) (Dec. 2022) 22109, https://doi.org/10.1038/s41598-022-24818-x.
[67] T.D.M. Florian, et al., Chemical composition analysis and structural features of banana rachis lignin extracted by two organosolv methods, Ind. Crop. Prod. 132 (Jun. 2019) 269–274, https://doi.org/10.1016/j.indcrop.2019.02.022.
[68] T.A. Salih, K.T. Hassan, S.R. Majeed, I.J. Ibraheem, O.M. Hassan, A.S. Obaid, In vitro scolicidal activity of synthesised silver nanoparticles from aqueous plant extract against Echinococcus granulosus, Biotechnology Reports 28 (Dec. 2020) e00545, https://doi.org/10.1016/j.btre.2020.e00545.
[69] S.D. Bhinge, et al., Formulation development and evaluation of antimicrobial polyherbal gel, Ann. Pharm. Fr. 75 (5) (Sep. 2017) 349–358, https://doi.org/10.1016/j.pharma.2017.04.006.
[70] M.A. Bhutkar, D.S. Randive, G.H. Wadkar, S.Y. Kamble, S. Bhinge, Formulation and evaluation of polyherbal gel containing extracts of Azadirachta indica, Adhatoda vasica, Piper betle, Ocimum tenuiflorum and Pongamia pinnata, jrp 23 (1) (Nov. 2018) 44–54, https://doi.org/10.12991/jrp.2018.107.